AC susceptibilities and relaxation time distributions for the two-dimensional and three-dimensional +or-J Ising spin glasses

1991 J. Phys.: Condens. Matter 3 3139

(http://iopscience.iop.org/0953-8984/3/18/008)

J. Phys.: Condens. Matter 3 (1991) 3139–3154. Printed in the UK

AC susceptibilities and relaxation time distributions for the two-dimensional and three-dimensional $\pm J$ Ising spin glasses

Masaki Suzuki, Takayuki Shirakura and Sakari Inawashiro
Department of Applied Physics, Tohoku University, Sendai, Japan

Received 7 August 1990, in final form 2 January 1991

Abstract. By means of two different methods in a Monte Carlo simulation, we calculate the AC susceptibilities $\chi(\omega)$ and relaxation time distributions $g(\tau)$ in the $\pm J$ Ising two-dimensional (2D) and three-dimensional (3D) spin glasses. The data obtained by the two methods separately are confirmed to be consistent with each other through the fluctuation dissipation theorem $\chi(\omega) = (1/T)\int d\tau\, g(\tau)/(1 - i\omega\tau)$. The imaginary parts $\mathrm{Im}\,\chi$ of the AC susceptibilities show a characteristic difference in the 2D and 3D spin glasses; as the frequency of the AC field is decreased, the height of the peak of $\mathrm{Im}\,\chi$ becomes higher in the 2D spin glass, and lower in the 3D spin glass. We can also see a difference between the $g(\tau)$ distributions in the 2D and 3D spin glasses, reflected by the difference in the $\chi(\omega)$-values. In the 3D spin glass, $\mathrm{Im}\,\chi$ has no frequency dependence at low temperatures, suggesting that the fluctuation spectrum of the magnetization shows $1/f$-noise behaviour in the spin-glass phase.

1. Introduction

There have been many theoretical and experimental studies on spin glasses (for a review, see Binder and Young (1986)). At present, it has been confirmed that the three-dimensional (3D) spin glass has a finite critical temperature ($T_c \neq 0$) (Ogielski and Morgenstern 1985) while the two-dimensional (2D) spin glass has a phase transition only at $T_c = 0$ (Morgenstern and Binder 1980). However, the physical properties are not well known, except for the mean-field model (Sherrington and Kirkpatrick 1975, Parisi 1980, 1983). It is important to investigate the dynamical properties in 2D and 3D spin glasses.

Murani (1981) indirectly measured a relaxation time distribution $g(\tau)$ by neutron inelastic scattering of the CuMn spin glass and showed that $g(\tau)$ is extended towards longer relaxation times at low temperatures. As for the AC susceptibility $\chi(\omega)$, many experiments have been performed. Huser *et al* (1986) studied $\chi(\omega)$ for spin glasses ($T_c \neq 0$) and superparamagnets ($T_c = 0$) and found a characteristic difference between their imaginary parts. They obtained $g(\tau)$ distributions from $\chi(\omega)$-values through the Cole–Cole plot. It was suggested that the relaxation time distribution $\hat{g}(\ln \tau)$ expressed on a logarithmic time scale shows a remarkable difference in the temperature dependence of the peak width in regions of slower relaxation times; the peak width of the spin glass increases as temperature T decreases, while that of the superparamagnets shows no temperature dependence.

0953-8984/91/183139 + 16 $03.50

In this paper, we concentrate on the AC susceptibility $\chi(\omega)$ and the relaxation time distribution $g(\tau)$ and try to find the characteristic features of the dynamical properties of 2D and 3D $\pm J$ Ising spin glasses. We investigate using Monte Carlo (MC) simulations whether or not similar differences to those found by Huser *et al* can be observed in the 2D and 3D $\pm J$ Ising spin glasses. We use two different methods in the MC simulation more suitable for calculations of $\chi(\omega)$ and $g(\tau)$, respectively (the details of the methods will be described in sections 2 and 3, separately). The effective algorithm of the MC simulation for ferromagnets used by Ito and Kanada (1988) was adapted to the $\pm J$ Ising model with an external AC field. The spin-flip probability follows the heat bath method.

In section 2 the AC susceptibilities $\chi(\omega)$ are calculated by a MC simulation in an external AC field. In section 3, autocorrelation functions for each spin are calculated, and the relaxation time distributions $g(\tau)$ are derived from these results. It is shown that the $g(\tau)$ distributions obtained in section 3 are consistent with the $\chi(\omega)$-values in section 2 through the fluctuation dissipation theorem (FDT). Section 4 contains a discussion and summary.

Before going into detailed calculations, let us define the relaxation time distribution $g(\tau)$. $g(\tau)$ is related to an autocorrelation function of the total magnetization $M(t) \equiv \sum_{i=1}^{N} S_i(t)$ (where $S_i(t)$ is a spin at time t and at a site i and N is the number of spins), as follows:

$$C(t) \equiv [\langle M(0)M(t)\rangle]_{\mathrm{av}} = N\int_0^\infty \mathrm{d}\tau\, g(\tau)\exp\left(\frac{-|t|}{\tau}\right) \tag{1}$$

where the thermal and configurational averages are denoted by $\langle \ldots \rangle$ and $[\ldots]_{\mathrm{av}}$, respectively. Using the FDT, the imaginary part $\mathrm{Im}[\chi(\omega)]$ of the susceptibility is expressed by $g(\tau)$:

$$\mathrm{Im}[\chi(\omega)] = \frac{\omega}{2T}C(\omega) \equiv \frac{\omega}{2T}\int_{-\infty}^{\infty} \mathrm{d}t \exp(\mathrm{i}\omega t)\, C(t)$$

$$= \frac{N}{T}\int_0^\infty \frac{\mathrm{d}\tau\, g(\tau)\omega\tau}{1+(\omega\tau)^2}. \tag{2}$$

Making use of the Kramers–Kronig relation, the susceptibility $\chi(\omega)$ is given by

$$\chi(\omega) = \frac{N}{T}\int_0^\infty \frac{\mathrm{d}\tau\, g(\tau)}{1-\mathrm{i}\omega\tau}. \tag{3}$$

On the other hand, we can rewrite $C(t)$ as

$$[\langle M(0)M(t)\rangle]_{\mathrm{av}} = \sum_i [\langle S_i(0)S_i(t)\rangle]_{\mathrm{av}} + \sum_{\substack{i,j \\ i\neq j}} [\langle S_i(0)S_j(t)\rangle]_{\mathrm{av}}. \tag{4}$$

Because the second term on the right-hand side of (4) vanishes in the $\pm J$ model with equal probabilities of $\pm J$ bonds studied in this paper, we obtain from (1) and (4)

$$\frac{1}{N}\sum_i [\langle S_i(0)S_i(t)\rangle]_{\mathrm{av}} = \int_0^\infty \mathrm{d}\tau\, g(\tau)\exp\left(\frac{-|t|}{\tau}\right). \tag{5}$$

We use this relation to determine $g(\tau)$ from the autocorrelation functions of each spin in section 3.

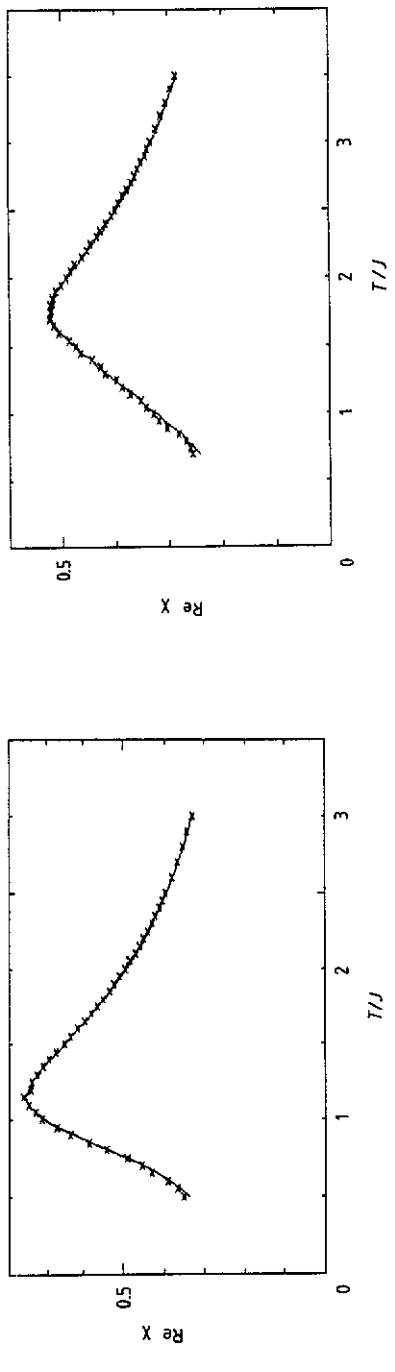

Figure 1. Re χ and Im χ versus T with $i_2 = 24\,000$ (×) and 96 000 (——) (*a*) in the 2D system and (*b*) in the 3D system.

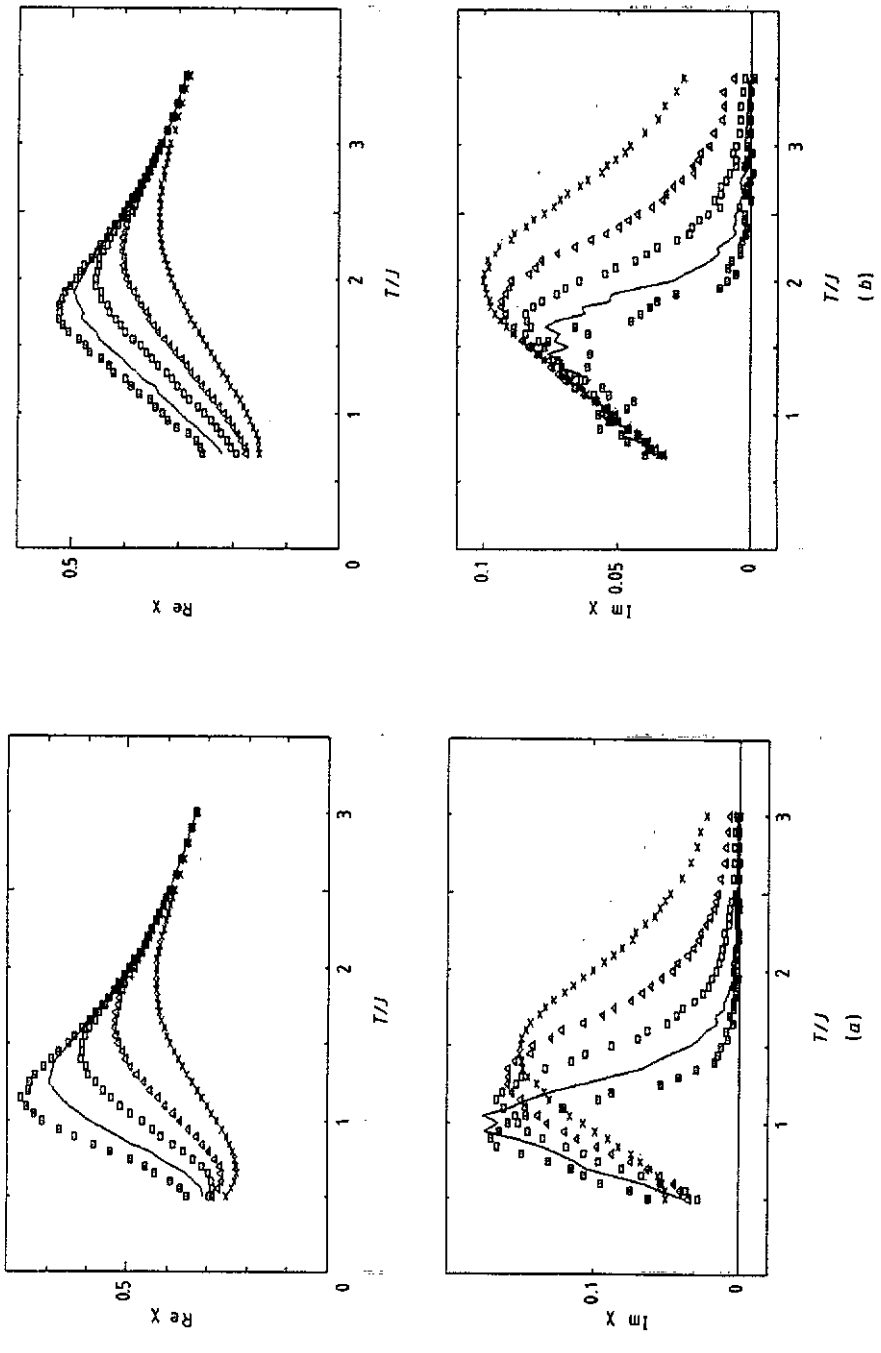

Figure 2. Re χ and Im χ versus T at $n_{\text{cyt}} = 6000$ (□), 2000 (——), 600 (□), 200 (△), 60 (×) and 20 (· · · ·) (*a*) in the 2D system and (*b*) in the 3D system.

2. The AC susceptibilities

In this section we calculate the AC susceptibilities for several frequencies by a MC simulation in an external AC field (Shirakura *et al* 1987) for the 2D and 3D $\pm J$ Ising spin glasses. The Hamiltonian is given by

$$H = -\sum_{\langle ij \rangle} J_{ij} S_i S_j - h_{\text{ext}} \sum_i S_i \qquad S_i = \pm 1$$
$$P(J_{ij}) = \tfrac{1}{2}[\delta(J_{ij} - J) + \delta(J_{ij} + J)] \tag{6}$$

where the distribution of the interactions J_{ij} is denoted by $P(J_{ij})$. The external AC field is applied as follows: at the ith MC step per spin (MCS) the external field is taken to be $h_{\text{ext}} = \delta h \cos[(i-1)\omega]$, where $\omega = 2\pi/n_{\text{cycl}}$; n_{cycl} is a positive integer. After i_1 MCSs are discarded to achieve a stationary state, data for $i_2 - i_1$ MCSs are kept for a Fourier analysis of the magnetizations. Shirakura *et al* (1987) applied this method to ferromagnets and obtained the AC susceptibilities as expected.

The parameters used in this section are determined as follows. For financial reasons, we fix the number of spins at $N = 50 \times 50$ for the 2D system and $N = 14 \times 14 \times 14$ for the 3D system. The number of samples with different bond configurations is chosen to be 32. The other available parameters are the amplitude δh, the number n_{cycl} of cycles of an AC field and the numbers i_1, i_2 of MCSs, and they will be chosen as follows.

First we consider the field amplitude δh. We want to choose δh as small as possible but owing to the finiteness of N, when $\delta h/J \langle N^{-1/2} (\simeq 0.02)$, the scatter of the data become relevantly large. We choose $\delta h = 0.1\,J$ for which the scatter of the data is small and the effect of the finiteness of δh is irrelevant.

Next we choose the numbers n_{cycl} of cycles of an AC field. There will be an upper limit for n_{cycl} owing to the finiteness of N, because we cannot measure correctly a susceptibility with a longer cycle than the time scale on which spin clusters with N spins fluctuate. In order to estimate this time scale roughly, we refer to figure 9 in the paper by Ogielski (1985) where the spin autocorrelation functions for $N = 8^3$, 16^3 and 32^3 are plotted against the time difference. The data for $N = 16^3$ deviate from those for $N = 32^3$ when the time difference exceeds 10^5 MCSs. Because the size treated in this section ($N = 14^3$ or 50^2) is a little smaller than $N = 16^3$, we limit ourselves to $n_{\text{cycl}} < 10^4$ for safety. We choose the next six values, $n_{\text{cycl}} = 20, 60, 200, 600, 2000$ and 6000.

Finally we choose the numbers i_1, i_2 of MCSs. Figures 1(a) and 1(b) show the susceptibilities (Re χ and Im χ) versus temperature T, with $i_2 = 24\,000$ and 96 000 in the 2D and 3D systems, respectively, when $i_1 = n_{\text{cycl}} = 6000$. All data in this paper are always calculated with decreasing T. In the 2D system, the data for $i_2 = 24\,000$ are almost in agreement with those for $i_2 = 96\,000$. In the 3D system, scatter of the data, especially of Im χ, for $i_2 = 24\,000$ is distinctly larger than for $i_2 = 96\,000$, but we do not find a systematic shift between them. Therefore $i_1 = 6000$ and $i_2 = 24\,000$ were chosen. (The scatter of the data with a smaller n_{cycl} is always smaller than that with $n_{\text{cycl}} = 6000$.)

In figure 2 are shown the susceptibilities in the 2D and 3D $\pm J$ spin glasses for these values of the parameters. As for Re χ, the peak position shifts to lower temperatures and its height becomes higher for both the systems as the frequency $\omega = 2\pi/n_{\text{cycl}}$ is decreased. We find a characteristic difference between their Im χ. As the frequency is decreased, the peak position of Im χ shifts to lower temperatures for both the systems, while its height becomes higher for the 2D system and lower for the 3D system. These behaviours are similar to those seen in the experiments on the superparamagnets ($T_c =$

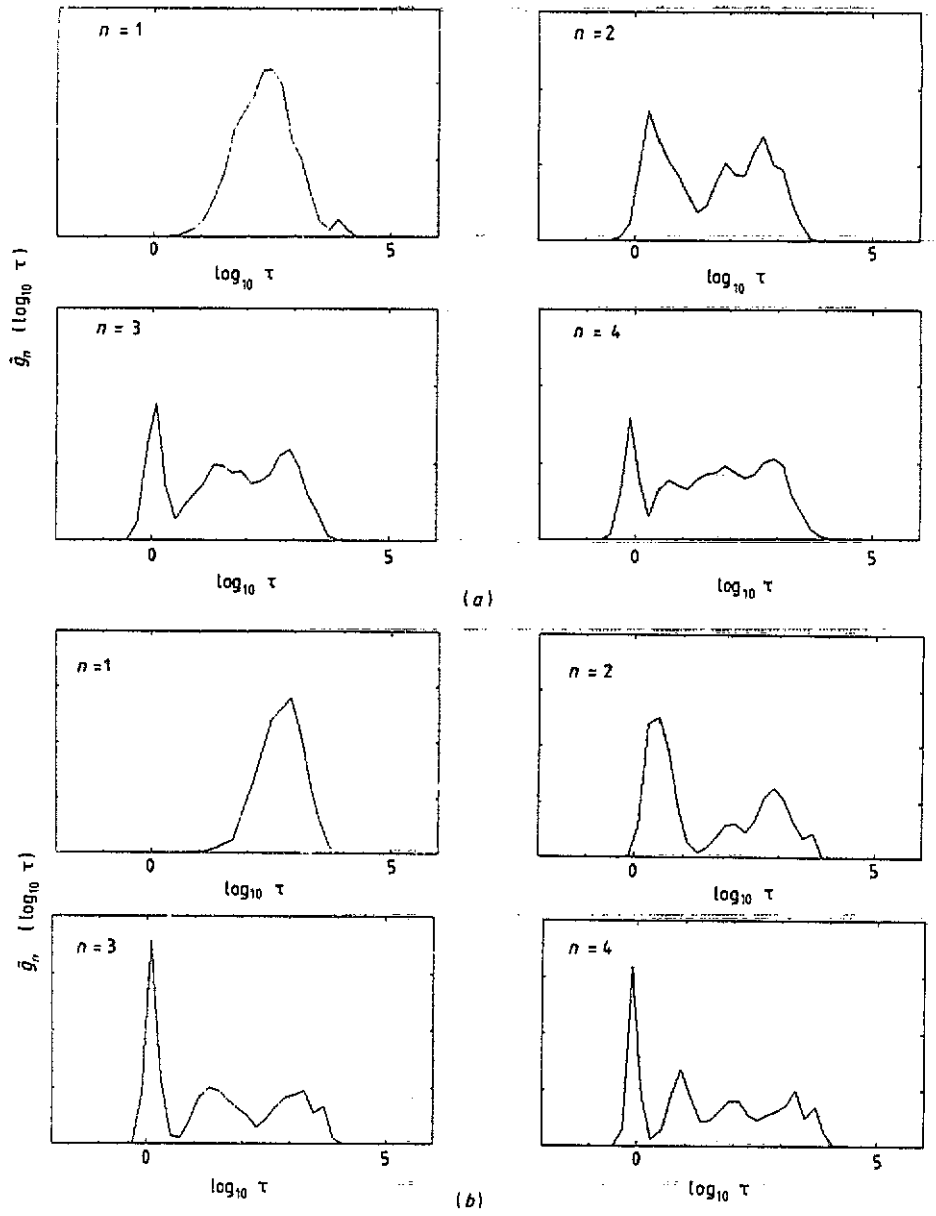

Figure 3. $\tilde{g}_n(\log_{10}\tau)$ versus $\log_{10}\tau$ with $n = 1, 2, 3$ and 4 (*a*) at $T = 1.1J$ in the 2D system and (*b*) at $T = 1.6J$ in the 3D system. The ordinate on the vertical axis is in arbitrary units which are the same for all n-values.

0) and on the spin-glass materials ($T_c \neq 0$) (Huser *et al* 1986, Dekker *et al* 1989, Gunnarsson *et al* 1988), respectively. This difference in the ω-dependence of Im χ suggests a qualitative difference in relaxation phenomena in the high-temperature phase between a spin glass with $T_c = 0$ and a spin-glass with $T_c \neq 0$. Huser *et al* (1986) studied the relaxation time distribution $g(\tau)$ from the Cole–Cole plot of the AC susceptibility $\chi(\omega)$. In the next section we evaluate $g(\tau)$ in a more direct manner in which we calculate autocorrelation functions for each spin.

Finally in this section, we note in figure 2(*b*) that values of Im χ with different ω-values in the 3D spin glass converge to a single line at low temperatures. This suggests that the values of Im χ have no ω-dependence in the low-temperature (spin-glass) phase. If this is true, the fluctuation spectrum of the magnetization in this model exhibits $1/f$-noise behaviour in the spin-glass phase, because $C(\omega) = (2T/\omega)\,\mathrm{Im}[\chi(\omega)]$ as easily seen from (2). It is an interesting problem whether or not this $1/f$-noise behaviour is to be attributed to a self-similarity of the free-energy structure in the spin-glass phase of the 3D spin glass. On the other hand, our results in figure 2(*a*) show that the spectrum in the 2D spin glass never exhibits $1/f$-noise behaviour, contrary to the results of Marinari *et al* (1984).

3. Relaxation time distributions

In this section we determine the relaxation time distribution $g(\tau)$ by a direct method in the MC simulation without an external field. We want to know whether or not we can see a qualitative difference between the $g(\tau)$ for the 2D and 3D systems similar to that between the superparamagnets ($T_c = 0$) and the spin-glass materials ($T_c \neq 0$) which was predicted by Huser *et al* (1986) from the $\chi(\omega)$-values. (It is confirmed that the $g(\tau)$ distributions obtained here are consistent with the $\chi(\omega)$-values in section 2 through the FDT (3).)

We use the method of Nemoto and Takayama (1983) to determine $g(\tau)$ by a MC simulation (for the 1D spin glass, $g(\tau)$ has been calculated by Kumar and Stein (1980)). The number N of spins and the number N_s of samples are fixed such that $N = 32 \times 32$ and $N_s = 8$ for the 2D system, and $N = 16 \times 16 \times 32$ and $N_s = 1$ for the 3D system. The total number of spins is $N \times N_s = 8192$ for both systems. We calculate the auto-correlation functions for each spin:

$$C_i(t) = \langle S_i(0)S_i(t)\rangle = \frac{1}{m}\sum_{l=1}^{m} S_i(l)S_i(l+t) \tag{7}$$

in an equilibrium state at temperature T. Nemoto and Takayama (1983) fitted $C_i(t)$ in the 2D Gaussian spin glass to the following double-exponential function:

$$C_i(t) = p_i \exp(-t/\tau_{1i}) + (1 - p_i)\exp(-t/\tau_{2i})$$

and obtained the relaxation time distribution

$$g(\tau) = \frac{1}{N}\sum_i [p_i\delta(\tau - \tau_{1i}) + (1 - p_i)\delta(\tau - \tau_{2i})]. \tag{8}$$

Because results obtained by a double-exponential fitting are not satisfactorily consistent with the $\chi(\omega)$-values in section 2 (especially in the 3D system) as seen in the following, we tried to fit $C_i(t)$ to n-exponential functions with $n = 1, 2, 3$ and 4.

First the system is cooled in the range $T_i \geq T \geq T_{m2}$ with a temperature difference $\Delta T = 0.1\,J$ and 6000 MCSs at each temperature. In the range $T_{m1} \geq T \geq T_{m2}$, after 6000 MCSs are discarded to equilibrate the system at each temperature, the $C_i(t)$-values for 36 points of t ($\leq$6000) with $m = 20\,000$ are measured. In the range $T_{m2} - 0.05\,J \geq T \geq T_f$, the system is gradually cooled with $\Delta T = 0.05\,J$ and 100 000 MCSs at each temperature. At alternate temperatures, after 100 000 MCSs are discarded to equilibrate the system, the $C_i(t)$-values for 46 points of t ($\leq$60 000) with $m = 300\,000$ are measured. We choose

$(T_i, T_{m1}, T_{m2}, T_f) = (3.0J, 2.0J, 1.5J, 0.8J)$ for the 2D system and $(3.5J, 2.5J, 2.0J, 1.2J)$ for the 3D system. Values of t are chosen such as

$$t = 1, 2, 3, 4, 5, 6, 7, 8, 10, 12,$$

$$15, 20, 30, 40, 50, 60, 70, 80, 100, 120,$$

$$\ldots$$

$$\ldots \qquad , 12\,000,$$

$$15\,000, 20\,000, 30\,000, 40\,000, 50\,000 \text{ and } 60\,000.$$

Hereafter we study the distribution of $\log_{10}\tau$, $\hat{g}(\log_{10}\tau)$, rather than $g(\tau)$.

Except for the single-exponential fitting, the n-exponential fittings are not necessarily successful for all spins. The successful rate becomes worse with increasing n. In table 1 are shown the numbers of spins for which the n-exponential fitting failed in the 2D and 3D systems, respectively. For the three- and four-exponential fittings, the successful rates

Table 1. The numbers of spins for which the n-exponential fitting failed in the 2D system and in the 3D system. The total number of spins is $N \times N_s = 8192$ for both systems.

	Number of spins for which the n-exponential fitting failed		
T/J	$n = 2$	$n = 3$	$n = 4$
	2D system		
2.0	26	4544	8132
1.9	12	4400	8026
1.8	3	3535	7972
1.7	3	2875	7804
1.6	1	2309	7585
1.5	0	1817	7310
1.4	0	293	3465
1.3	0	256	2791
1.2	1	322	2777
1.1	4	386	2273
1.0	29	690	2560
0.9	114	1118	2605
0.8	485	2060	3557
	3D system		
2.5	1	2654	7932
2.4	0	2228	7827
2.3	1	1414	7411
2.2	0	899	7122
2.1	0	623	6525
2.0	0	376	5851
1.9	0	3	1167
1.8	0	3	751
1.7	0	23	600
1.6	1	44	881
1.5	0	78	827
1.4	31	224	1163
1.3	88	944	2239
1.2	202	1270	2640

change discontinuously at temperature T_{m2} where we changed the average number m for $C_i(t)$. In order to calculate $\hat{g}_n(\log_{10}\tau)$, we used values obtained by the $(n-1)$-exponential fitting for the spins for which the n-exponential fitting failed. In figure 3 are shown typical examples of $\hat{g}_n(\log_{10}\tau)$ in the 2D and 3D systems obtained by the n-exponential fittings with $n = 1$, 2, 3 and 4. We can see from figure 3 that $\hat{g}_n(\log_{10}\tau)$ appears to approach a true distribution with increasing n, favouring a graph with n peaks.

Comparisons of $\chi(\omega)$ in section 2 (we denote them as $\chi_{si}(\omega)$ hereafter) with $\chi(\omega)$ calculated from the relaxation time distributions through (3) (we denote them as $\chi_{cal}^{(n)}(\omega)$ hereafter) are shown in figures 4 and 5. The $\chi_{cal}^{(4)}(\omega)$-values obtained by the four-exponential fitting are in good agreement with $\chi_{si}(\omega)$-values for $n_{cycl} > 200$. The $\chi_{cal}^{(1)}(\omega)$-values largely deviate from the $\chi_{si}(\omega)$-values below a temperature $T_p(\omega)$ at which $\mathrm{Re}[\chi_{si}(\omega)]$ shows a peak because, at low temperatures, part of the fast relaxation cannot be treated correctly by the single-exponential fitting. The disagreement between $\chi_{si}(\omega)$ and $\chi_{cal}^{(4)}(\omega)$ for $n_{cycl} \leqslant 200$ may be due to the effect of a discrete cyclic change in an external field in the measurement of $\chi_{si}(\omega)$, rather than to the effect of the n-exponential fitting. We discuss this in section 4.

Therefore we expect that the $\hat{g}_4(\log_{10}\tau)$ distributions obtained by the four-exponential fitting are the best of all the approximations available now. In figure 6 are shown $\hat{g}_4(\log_{10}\tau)$ distributions in the 2D and 3D systems at several temperatures. At high temperatures, the $\hat{g}_4(\log_{10}\tau)$ distributions of the 3D system are almost in agreement with those of the 2D system at temperatures about $0.5J$ lower than the 3D system. However, as the temperature is lowered, characteristic differences between the 2D and 3D systems appear: in the 2D system, $\hat{g}_4(\log_{10}\tau)$ has a two-peak structure even at low temperatures. On the other hand, in the 3D system the slow part of $\hat{g}_4(\log_{10}\tau)$ seems to become a rectangular distribution. Here we define the boundary between the slow part and the fast part as the minimum point of $\hat{g}_4(\log_{10}\tau)$ in the range $1 \geqslant \log_{10}\tau \geqslant 0$. The ratio of the fast part to the slow part is larger in the 3D system than in the 2D system at temperatures about $0.5J$ lower than the 3D system.

4. Discussion

First we discuss the effect of discrete cyclic changes of the external field in the calculation of $\chi_{si}(\omega)$ which might be the reason for the disagreement between $\chi_{si}(\omega)$ and $\chi_{cal}(\omega)$ for $n_{cycl} \leqslant 200$. The spin-flip probability of the MC simulation performed in sections 2 and 3 follows the heat bath method. Here we compare $\chi_{si}(\omega)$ in section 2 with $\chi_{si}(\omega)$ obtained by the Metropolis method. It is known from a study of critical relaxational phenomena for ferromagnets (Ito 1988) that a time scale of 1 MCS in the Metropolis method is about three times that in the heat bath method. Then in figure 7 we compare $\chi_{si}(\omega)$ for $n_{cycl} =$ 6000, 2000, 600, 200 and 60 in the heat bath method with $\chi_{si}(\omega)$ for $n_{cycl} = 2000$, 600, 200, 60 and 20 in the Metropolis method. These values agree very well for $n_{cycl} \geqslant 600$ (on the time scale of the heat bath method) but, when $n_{cycl} \leqslant 200$, $|\chi_{si}^{M}(\omega) - \chi_{si}^{HB}(\omega)|$ becomes large as n_{cycl} decreases. It seems that this disagreement is due to the effect of the discretization of time.

Next we discuss the temperature dependence of the averaged relaxation time $\tau_{av} \equiv \int_0^\infty \mathrm{d}\tau\, \tau g(\tau)$. Ogielski (1985) indicated that another characteristic relaxation time $\hat{\tau} \equiv \int_0^\infty \mathrm{d}\tau\, \tau^2 g(\tau) / \int_0^\infty \mathrm{d}\tau\, \tau g(\tau)$ is relevant for the observable relaxational phenomena. However, the $\hat{\tau}$-values obtained from $\hat{g}_4(\log_{10}\tau)$ in section 3 have a larger scatter than the τ_{av}-values do. Therefore we concentrate on τ_{av} only. The values of τ_{av} calculated

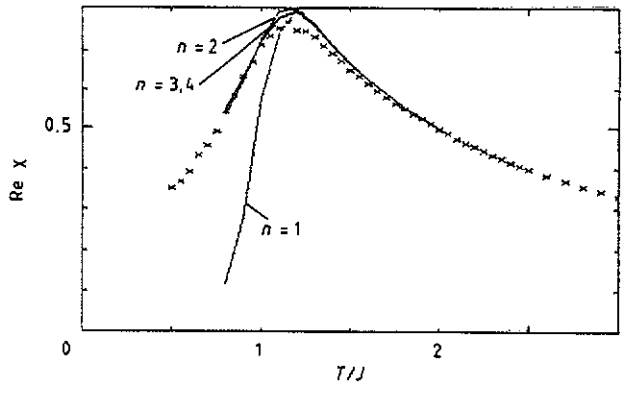
n = 2
n = 3,4
n = 1
Re χ
0.5
0
1
2
T/J

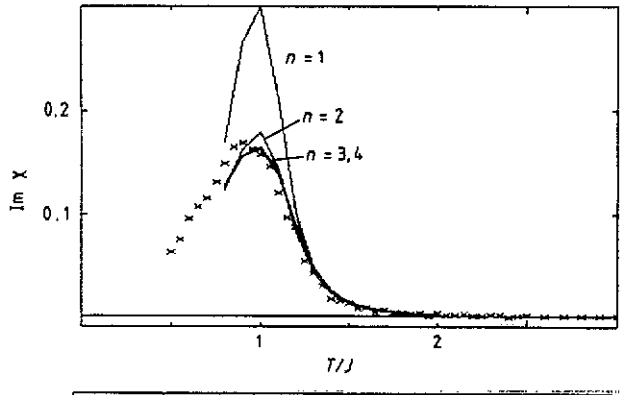
n = 1
n = 2
n = 3,4
Im χ
0.2
0.1
1
2
T/J

(a)

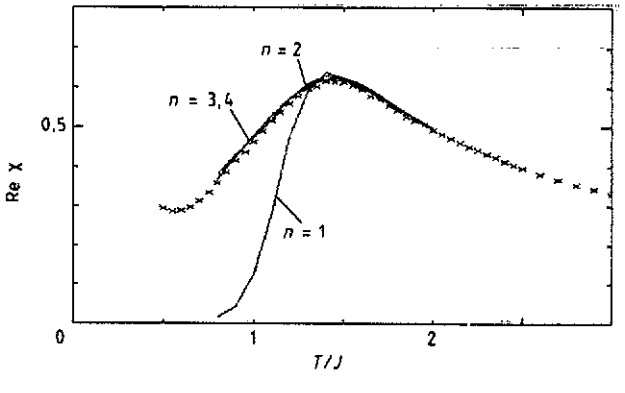
n = 2
n = 3,4
n = 1
Re χ
0.5
0
1
2
T/J

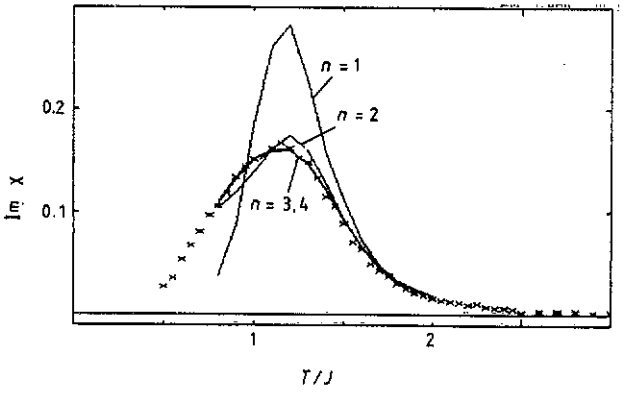
n = 1
n = 2
n = 3,4
Im χ
0.2
0.1
1
2
T/J

(b)

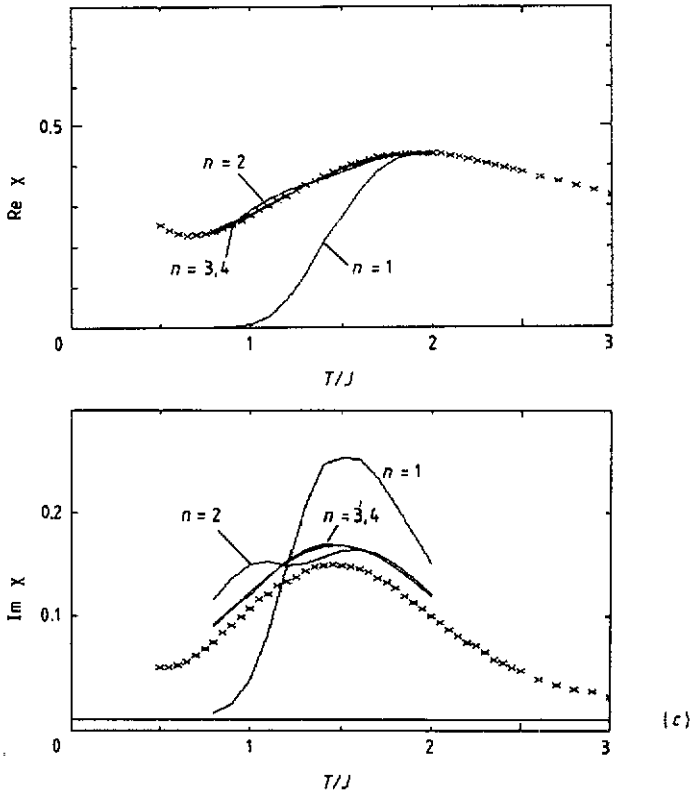

Figure 4. $\chi_{si}(\omega)$ (×) and $\chi_{cal}^{(a)}(\omega)$ (———) versus T in the 2D system at n_{cycl}-values of (*a*) 6000, (*b*) 600 and (*c*) 60.

from the $\hat{g}_4(\log_{10}\tau)$ distributions in the 2D and 3D systems are fitted to the following two functional forms (Binder and Young 1984, Ogielski 1985): the type (*a*) functional form is the generalized Arrhenius law $\tau_{av} = \tau_0 \exp[(E/T)^\sigma]$; the type (*b*) functional form is the power law $\tau_{av} = C_0(T - T_c)^{-z_{av}\nu}$, $T > T_c$. Because we measured the autocorrelation functions of spins with $t \leqslant 60\,000$, we use only the data for $\tau_{av} < 60\,000$. This is satisfied for $T \geqslant 0.9J$ in the 2D system and for $T \geqslant 1.4J$ in the 3D system. We perform six-point and ten-point fittings. In the six-point fitting, we use the data at $T/J = 0.9, 1.0, \ldots, 1.4$ in the 2D system and at $T/J = 1.4, 1.5, \ldots, 1.9$ in the 3D system. In the ten-point fitting, we use $T/J = 0.9, 1.0, \ldots, 1.8$ in the 2D system and $T/J = 1.4, 1.5, \ldots, 2.3$ in the 3D system. We define the magnitude of data scatter Δ for the two functional forms as follows: for the generalized Arrhenius law (type (*a*)),

$$\Delta \equiv \sum_i \frac{[\ln(\tau_{avi}) - \ln(\tau_0) - (E/T_i)^\sigma]^2}{\text{number of data points}}$$

and for the power law (type (*b*)),

$$\Delta \equiv \sum_i \frac{[\ln(\tau_{avi}) - \ln(C_0) + z_{av}\nu \ln(T_i - T_c)]^2}{\text{number of data points}}.$$

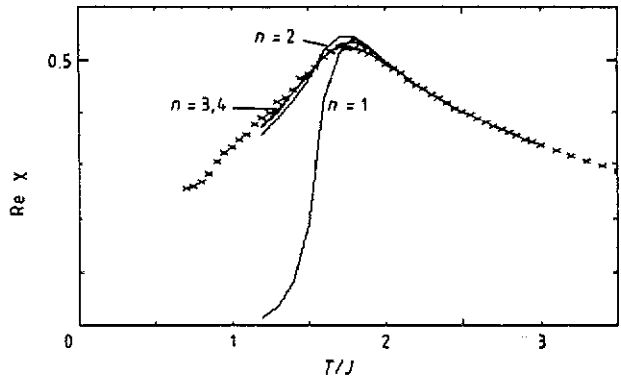
n = 2
n = 3,4
n = 1
0.5
Re χ
0
1
2
3
T/J

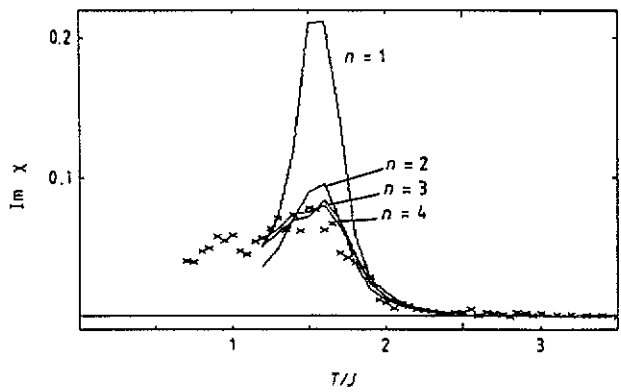
0.2
0.1
Im χ
n = 1
n = 2
n = 3
n = 4
1
2
3
T/J

(a)

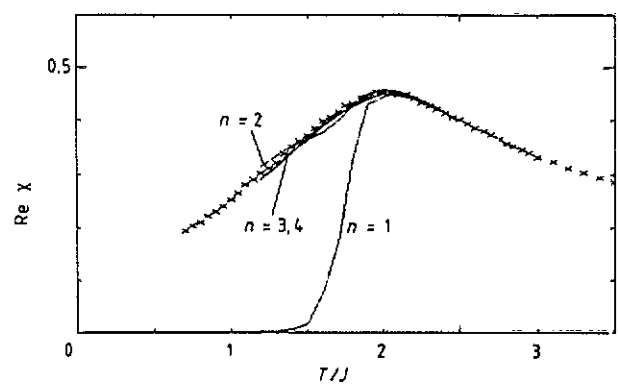
0.5
Re χ
n = 2
n = 3,4
n = 1
0
1
2
3
T/J

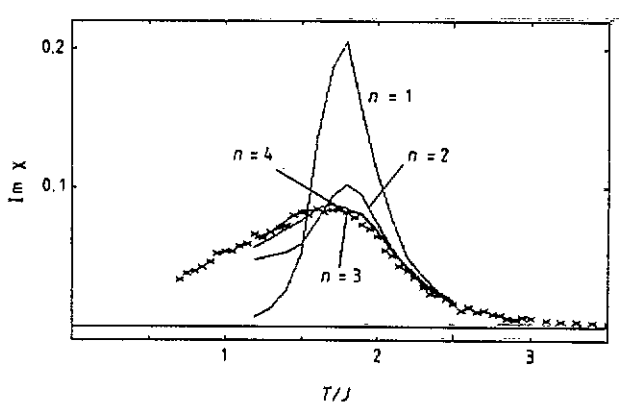
0.2
0.1
Im χ
n = 1
n = 4
n = 2
n = 3
1
2
3
T/J

(b)

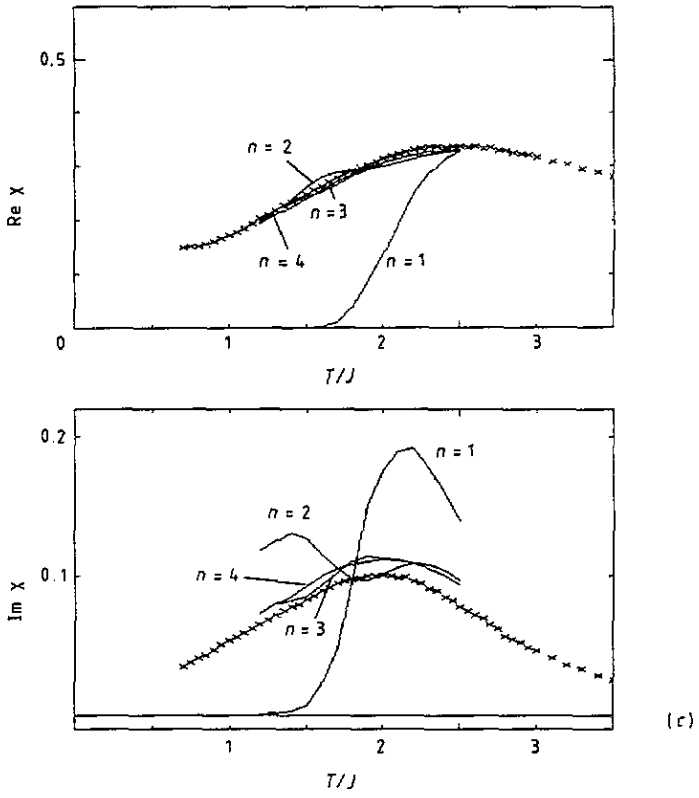

Figure 5. $\chi_{si}(\omega)$ (×) and $\chi_{cal}^{(n)}(\omega)$ (———) versus T in the 3D system at n_{cyc}-values of (*a*) 6000, (*b*) 600 and (*c*) 60.

By comparing Δ-values, we determine a suitable functional form of the temperature dependence of τ_{av} in the 2D and 3D systems, respectively.

The results in the 2D and 3D systems are as follows. For the 2D $\pm J$ model, type (*a*) function, ten-point fitting,

$$\sigma = 1.49 \qquad E = 4.51J \qquad \ln(\tau_0) = -2.14 \qquad \Delta = 0.0021.$$

For the 2D $\pm J$ model, type (*a*) function, six-point fitting,

$$\sigma = 1.22 \qquad E = 7.30J \qquad \ln(\tau_0) = -3.97 \qquad \Delta = 0.0022.$$

For the 2D $\pm J$ model, type (*b*) function, ten-point fitting,

$$T_c = 0.696J \qquad z_{av}\nu = 4.28 \qquad \ln(C_0) = 2.14 \qquad \Delta = 0.0067.$$

For the 2D $\pm J$ model, type (*b*) function, six-point fitting,

$$T_c = 0.596J \qquad z_{av}\nu = 5.54 \qquad \ln(C_0) = 2.30 \qquad \Delta = 0.0027.$$

For the 3D $\pm J$ model, type (*a*) function, ten-point fitting,

$$\sigma = 3.43 \qquad E = 2.74J \qquad \ln(\tau_0) = 0.383 \qquad \Delta = 0.0179.$$

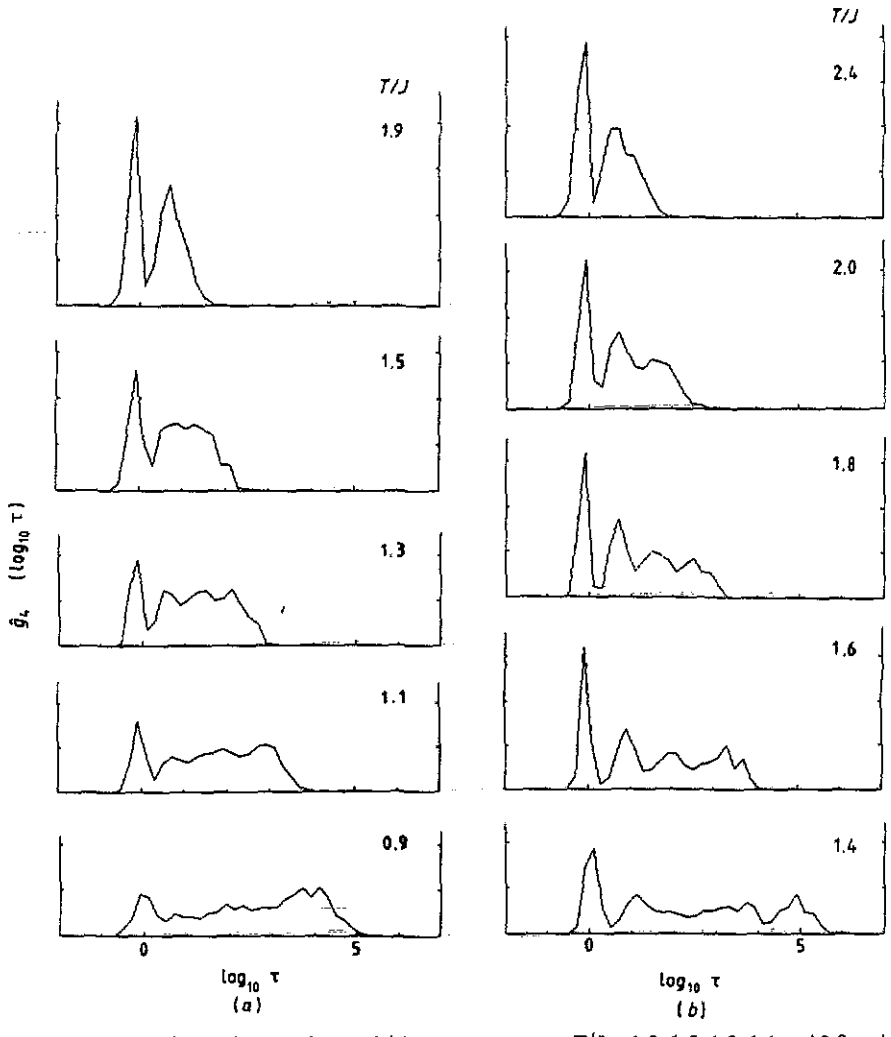

Figure 6. $\hat{g}_4(\log_{10}\tau)$ versus $\log_{10}\tau$ (*a*) in the 2D system at $T/J = 1.9, 1.5, 1.3, 1.1$ and 0.9 and (*b*) in the 3D system at $T/J = 2.4, 2.0, 1.8, 1.6$ and 1.4.

For the 3D $\pm J$ model, type (*a*) function, six-point fitting,

$$\sigma = 4.47 \qquad E = 2.27J \qquad \ln(\tau_0) = 1.82 \qquad \Delta = 0.0144.$$

For the 3D $\pm J$ model, type (*b*) function, ten-point fitting,

$$T_c = 1.29J \qquad z_{av}\nu = 3.83 \qquad \ln(C_0) = 2.11 \qquad \Delta = 0.0035.$$

For the 3D $\pm J$ model, type (*b*) function, six-point fitting,

$$T_c = 1.29J \qquad z_{av}\nu = 3.86 \qquad \ln(C_0) = 2.10 \qquad \Delta = 0.0046.$$

We can see by comparing values of Δ that the suitable functional forms are the generalized Arrhenius law (i.e. the type (*a*) function) for the 2D $\pm J$ model and the power law (i.e. the type (*b*) function) for the 3D $\pm J$ model. These results are consistent with previous investigations (see, e.g., Ogielski 1985). However, the parameter values for

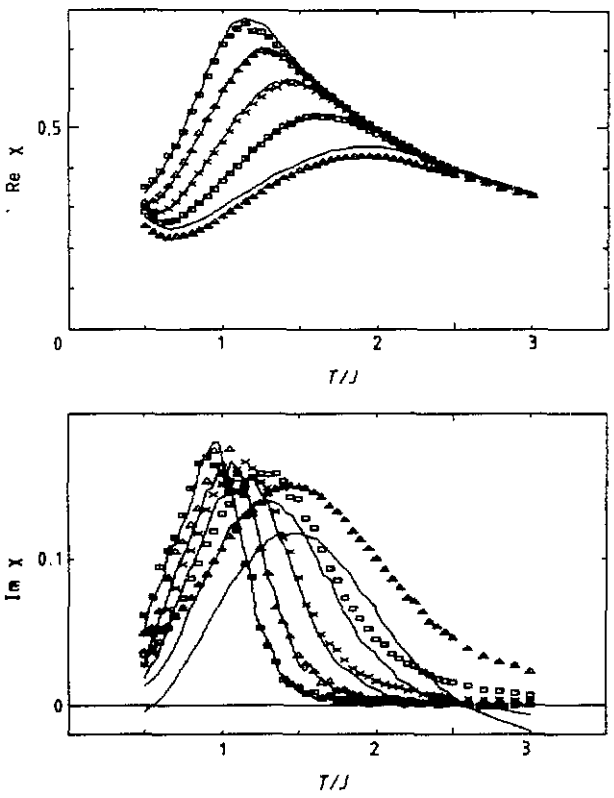

Figure 7. $\chi_{si}(\omega)$ versus T obtained by the Metropolis method (———) and by the heat bath method (n_{cycl} = 6000 (⊡), 2000 (△), 600 (×), 200 (□) and 60 (△)) in the 2D system. We also obtained similar results in the 3D system.

the type (a) function in the 2D system largely depend on the number of fitting points, and those for the type (b) function in the 3D system are different from Ogielski's values (T_c = 1.175 ± 0.025, $z_{av}\nu$ = 7.0 ± 0.8). These might be due to the shortness of the time span of MCS ($t \leqslant 60000$) and the small number of fitting points in this paper.

We think that the results in the paper are interesting for their qualitative properties, although further investigations should be performed to obtain good quantitative results for τ_{av} and so on. Sibani (1987) presented a model for spin glasses based on the picture of motion in phase space as thermally activated hopping in an ultrametric space and calculated AC susceptibilities. The frequency dependence of the AC susceptibility obtained by Sibani is similar to that of $\chi_{si}(\omega)$ in the 2D system, but not in the 3D system, in this paper. The difference between $\hat{g}_4(\log_{10}\tau)$ for the 2D and 3D systems might give some hints for suggesting a model which has AC susceptibilities similar to the $\chi_{si}(\omega)$ in the 3D system.

Acknowledgments

The authors would like to thank Professor F Matsubara for valuable discussions and encouragement. One of the authors (TS) would like to thank Professor H Takayama and Dr K Nemoto for valuable discussions.

References

Binder K and Young A P 1984 *Phys. Rev.* B **29** 2864
—— 1986 *Rev. Mod. Phys.* **58** 801
Dekker C, Arts A F M, de Wijn H W, van Duyneveldt A J and Mydosh J A 1989 *Phys. Rev.* B **40** 11243
Gunnarsson K, Svedlindh P, Nordblad P, Lundgren L, Aruga H and Ito A 1988 *Phys. Rev. Lett.* **61** 754
Huser D, van Duyneveldt A J, Nieuwenhuys G J and Mydosh J A 1986 *J. Phys. C: Solid State Phys.* **19** 3697
Ito N 1988 private communication
Ito N and Kanada Y 1988 *Supercomputer* **25** 31
Kumar D and Stein J 1980 *J. Phys. C: Solid State Phys.* **13** 3011
Marinari E, Paladin G, Parisi G and Vulpiani A 1984 *J. Physique* **45** 657
Morgenstern I and Binder K 1980 *Phys. Rev.* B **22** 288
Murani A P 1981 *J. Magn. Magn. Mater.* **22** 271
Nemoto K and Takayama H 1983 *J. Phys. C: Solid State Phys.* **16** 6835
Ogielski A T 1985 *Phys. Rev.* B **32** 7384
Ogielski A T and Morgenstern I 1985 *Phys. Rev. Lett.* **54** 928
Parisi G 1980 *J. Phys. A: Math. Gen.* **13** 1101
—— 1983 *Phys. Rev. Lett.* **50** 1946
Sherrington D and Kirkpatrick S 1975 *Phys. Rev. Lett.* **32** 1792
Shirakura T, Kajitani H and Inawashiro S 1987 *J. Phys. C: Solid State Phys.* **20** 6061
Sibani P 1987 *Phys. Rev.* B **35** 8572